



Institut für Numerische Simulation

Rheinische Friedrich-Wilhelms-Universität Bonn

Wegelerstraße 6 • 53115 Bonn • Germany
phone +49 228 73-3427 • fax +49 228 73-7527
www.ins.uni-bonn.de

M. Griebel, F. Heber

**A molecular dynamics study on
fullerene-implanted carbon nanotube as
electromagnetic sensing and emitting devices**

INS Preprint No. 0912

Oct 2009

A molecular dynamics study on fullerene-implanted carbon nanotori as electromagnetic sensing and emitting devices

Authors: Michael Griebel, Frederik Heber

Affiliations: Institute for Numerical Simulation, Wegelerstrasse 6,
53115 Bonn, Germany, heber@ins.uni-bonn.de

Abstract

Open-ended carbon nanotubes have been found to form toroidal structures [17]. These specific structures bear striking resemblance to electrographic coils. Two modes of action can be thought of: Either the metallic conductivity of certain chiralities of the nanotorus configuration is exploited directly or fullerenes may be implanted into the torus' inner region [10]. Alone these fullerenes are charge-neutral, but they may easily be inoculated with metals carrying additional charges. Henceforth, currents would not act upon the electrons in the nanotorus' surface but also on the fullerene's surplus charges. This interplay may lead to very interesting applications. We have investigated the mechanical stability of these toroidal systems by molecular dynamics simulation [6], employing a potential [1] well-suited for carbon. This research has significant importance on the frequency range and quality of applications employing nanotori as tunable circuits. We report on the current status of our findings.

1 Introduction

First discovery of torus-like structures has probably been by Liu et al. [17], then by Muster et al. [23] and Martel et al. [21, 22]. These purely accidental discoveries were followed by the discovery of coiling carbon nanotubes by acid treatment with ultrasound [21]. Since then both experimental and theoretical [12, 24] studies on carbon nanotori have been employed, with both concern to magnetic [29, 16]

and electric [31] effects. Colossal paramagnetic moments have been said to exist [18] for these structures, but remain unconfirmed.

The idea of using multi-walled nanotubes as gigahertz oscillators [8, 15] has been proposed. Hilder et al. suggested employing single atom [19, 10] and later C60 buckyballs [9] as oscillating particles. Tribological properties [20] and main sources of energy dissipation [32] of these oscillating nano-systems have been studied.

Furthermore, endohedral metallofullerenes have become a very active field of research and meanwhile can be produced with ease, Shinohara [26] gives a good overview. It is possible by x-ray defraction [28] or by electron energy-loss spectroscopy (EELS) [27] to confirm the endohedral nature of metallofullerenes. And they can be encapsulated in carbon nanotubes [11] and used to tune the electronic properties [14]. There are many applications such as using them as in-vivo radiotracers [2] besides their use in nanotubes and other nanostructures.

In order to increase the emitted or detected power an array of inoculated nanotori is imaginable. These nano-structures tend to phase-lock, which would be imperative for a collective reinforcement of the signal, a general tendency of non-linear interacting oscillators, see [13].

Hence, we note that all the basic capabilities are in place to produce metallofullerene-implanted carbon nanotubes, examine their successful construction and use them in electronic applications.

Tuzun et al. [30] suggested that fully dynamic and atomistic calculations of the flow of buckyballs inside nanotube structures should be employed. There-

fore, we investigate the mechanical properties of buckyballs orbiting inside nanotori by molecular dynamics simulations.

The remainder of the article is organised as follows: In section 2 we explain the numerical setup of the nano structures. In section 3 the performed experiments are described in detail. We end with a discussion of the findings in section 4.

2 Numerical procedures

We employ our parallel molecular dynamics software package TREMOLO [7] with empirical potentials according to Brenner [1] that has proven suitable for the simulation of covalently bonded carbon nanostructures, and which has been used before by the authors to calculate the mechanical strength of nanotubes embedded in polymers, see [5] for further details. Note that the atom count easily exceeds 100.000 atoms, hence a fully parallel implementation is essential for our investigations.

We construct single- and double-walled carbon nanotori by virtually coiling nanotubes on the xy plane, i. e. by a transformation to a toroidal coordinate system. Note that these nanotori can be defined by the length l of the initial nanotube and its chiral numbers (n, m) , see table 1 where we also give the initial nanotube's radius r that depends on (n, m) only. Note that the nanotorus' mean or central radius $R = \frac{l}{2\pi}$ can be easily inferred from the given circumference l which is nothing but the length of the original nanotube.

The time step width is $\Delta t = 0.1$ fs, initial velocities v_i are zero. The configurations are equilibrated at standard pressure and temperature. Total energies are computed in the NVE ensemble with constant particle number (N), constant volume (V) and constant energy (E). Molecular dynamics simulations are performed in the NVT ensemble, where the total energy is not conserved due to the action of a thermostat, keeping a constant temperature (T).

The embedded C_{60} buckyball is initially placed at $(R, 0, 0)$, where R is the radius of the nanotorus. It is set in motion by an initial force F_i acting for $t_i = 1.02$ fs in the y direction, given in table 1(a)

along with the resulting velocities of the buckyball structure in the y direction.

Simulations are subsequently performed for $T = 10.2$ ps to assess the initial stability of the moving buckyball inside the torus structure.

3 Calculations

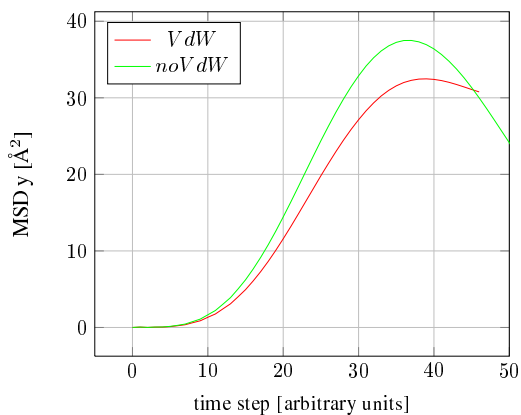
Our investigations are divided into three parts: First, we study whether the employed potential is suitable for the simulation of carbon nanotorus structure itself, that is if structures are stable and match with experimental constraints in terms of minimum stable torus' radii. Second, we embed a C_{60} buckyball inside the toroidal nanotube, driving it by an initial forced momentum along the torus' circumference. Therefrom, we determine the mechanical stability of the system in terms of friction and wall-buckyball collisions. Also the maximum possible velocity before destruction of the buckyball is approximated. Third, we attempt to look beyond the proposed scheme of the metallofullerene oscillators in terms of multi-wall nanotori setups and nanotori embedded in a polyethylene matrix. The latter would not only make the system more resistible against environmental effects, but also keep the tori itself in a fixed position, necessary for applications.

3.1 Nanotorus

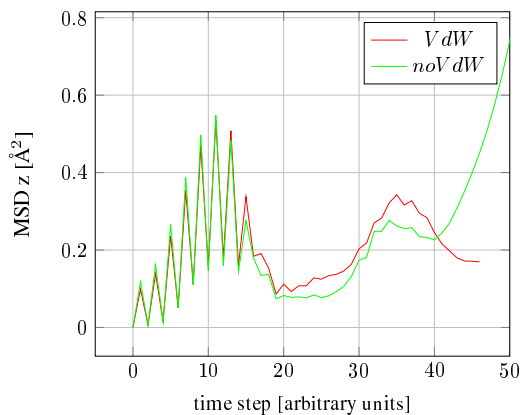
First, we investigate the stability of various $(16, x)$ carbon nanotorus configurations with regards to van der Waals-forces and radii. They are constructed without perturbations with a radius of 250\AA and subsequently equilibrated for 10.2 ps. During the simulation the mean square displacement $\|x - x_0\|_2$ of every atom with respect to its initial position x_0 is measured. This acts in the following as the central quantity for measuring stability.

3.1.1 Stable geometry

Van-der-Waals forces are important for multi-wall nanotubes, where a sliding inner tube will oscillate only due to the repelling Van-der-Waals force. It



1.1: y component of (16,0) torus



1.2: z component of (16,0) torus

Figure 1: Mean Square Displacement with respect to initial geometry: Van der Waals-forces play only a minor role with regards to the overall stability of the torus geometry, see figure 1.1. They are however essential when considering radial perturbations, see figure 1.2.

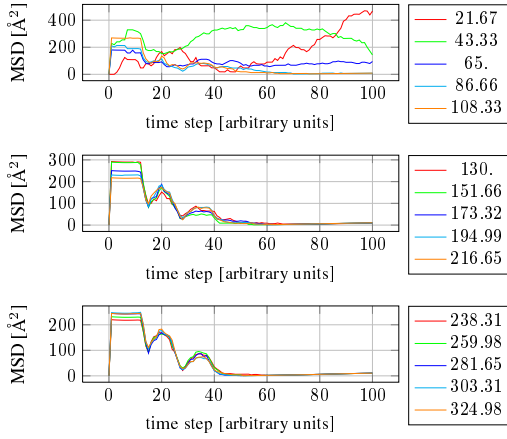
may easily be switched off by disabling the respective term in the Brenner potential. Thereby, we may study the equilibration phase with and without Van-der-Waals forces, measure the total mean square displacement of all atoms componentwise and hence the dependence of the single-wall nanotorus' stability on the Van-der-Waals forces. This is depicted in figure 1. We observe that Van-der-Waals forces are only significant for the radial deformations, given by the z component of the mean square displacement, see also similar observations by Ruoff et al. on nanotube deformations [25].

Next, we investigate nanotubes configurations $(16, x)$ with different lengths. The resulting different nanotorus' radii range from 10\AA up to 325\AA . In figure 2 the radial part or z component and one tangential, the y component, of the mean square displacement are depicted. The radial part allows for clear differentiation between stable and non-stable structures. For the $(16, 0)$ geometries we observe stability above $R = 100\text{\AA}$. A similar threshold can be found for the $(16, 8)$ geometries.

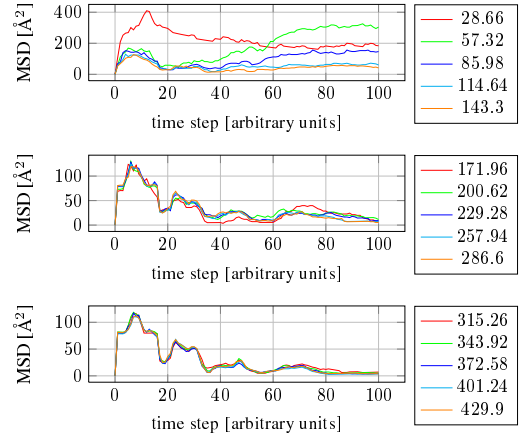
3.2 Nanotorus- C_{60} -oscillators

Having found that nanotorus configurations with radii above 100\AA are stable during equilibration, we continue on how the embedded and externally driven C_{60} buckyball interacts with the toroidal system. We employ the nanotorus geometries given in table 1. Note we now use a fixed nanotorus radius of $\approx 250\text{\AA}$ and give oscillating frequencies below with respect to this size.

First of all, we look at the force the buckyball feels from the surrounding torus' walls. In figure 3, we give the total energy of the system with the buckyball placed at various distances between the walls. The radii of each configuration was scaled to unity, hence the left-hand wall is located at 0 and the right-hand wall is located at 1. We note that there are in total two minima at ≈ 0.2 and at ≈ 0.8 , each in the vicinity of either wall and less than the interlayer graphene distance of 3.34\AA . Also, these are at the same scaled position, independent of chirality. The height of the potential barrier in between however differs with chirality and increases with increasing nanotube' radius r . These observations are in accordance with theoretical investigations by Cox et al. [3].



2.1: Mean Square radial Displacement (16,0) torus



2.2: Mean Square radial Displacement of (16,8) torus

Figure 2: The mean squared displacement between the initial (ideal) torus configuration and later stages for increasing torus' radii is shown. As can be seen, diameters below 100 Å are unstable and the geometry breaks apart. Note that this threshold depends on the chiral angle, as studied by Huhtala et al. [12].

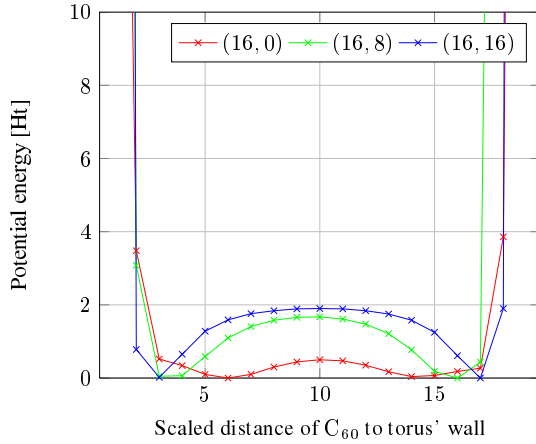
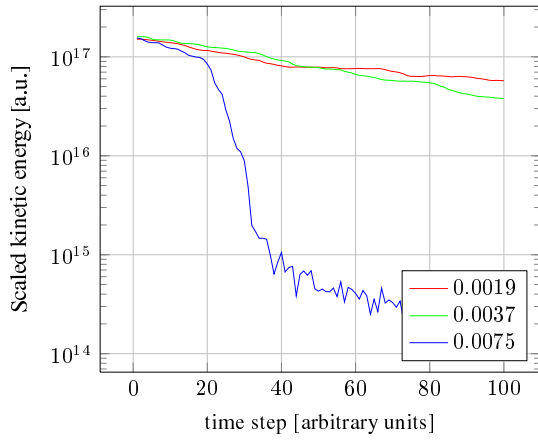


Figure 3: C_{60} experiences potential minima inside nanotube close to the wall, at distance less than the interlayer distance of graphene.

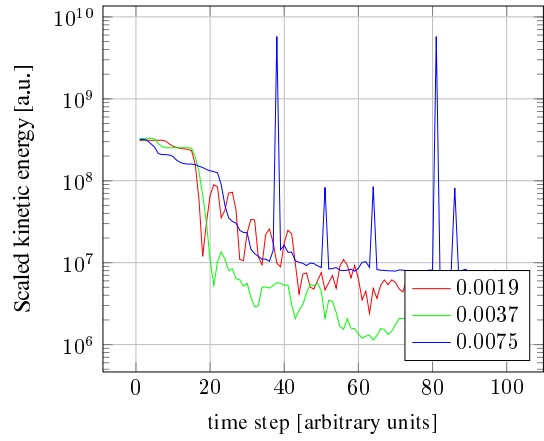
3.2.1 Kinetics of orbiting C_{60}

Second, we analyse the profiles of the dynamics of an orbiting C_{60} by looking at the behavior of the kinetic energy over time, depicted in figure 4¹. During the equilibration of 10.2 ps of the toroidal geometry the embedded buckyball is propelled by a force in the y direction of varying strength, see table 1(a). Therefrom we may derive upper limits on the possible velocity before the buckyball structure fails due to wall friction. We observe that this breakdown occurs at the limit of $\tau_v = 0.05$ Å/fs, or roughly 30 GHz, for the (16, 0) geometry, see figure 4.1. The (16, 8) behaves altogether very unstable and does not allow for a free orbiting of the buckyball, see figure 4.2. One possible explanation might be that the chiral nature of the (16, 8) configuration introduces an additional internal rotation preventing an orbiting path, similar to the helical structure of a gun barrel, stabilizing the bullet by an additional induced rotation. In figure 4.3 we give the velocity difference between subsequent timesteps. There are two regimes: If below τ_v , the change in velocity is in general small. If above τ_v ,

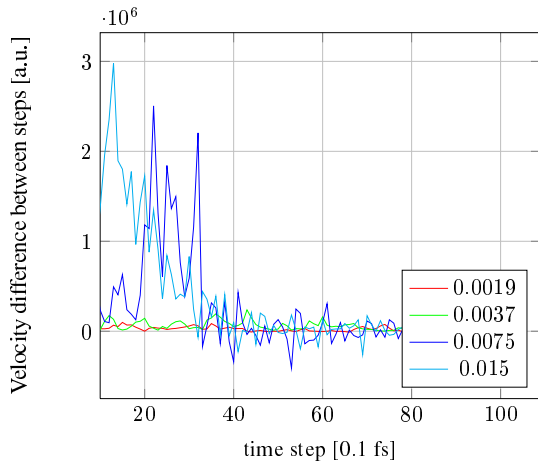
¹Note that the given kinetic energies in the following graphs were derived from a finite difference scheme and thus may contain irregular peaks.



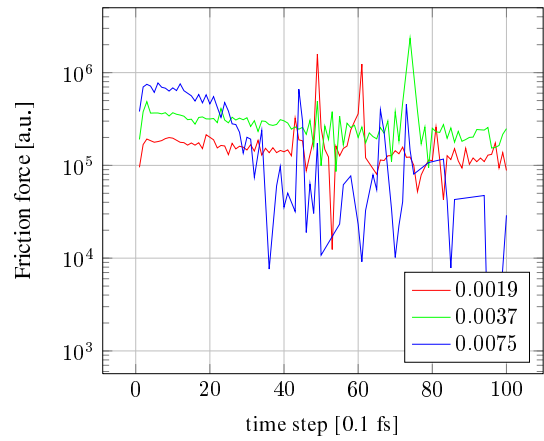
4.1: Kinetic energy of v_x for (16,0), scaled.



4.2: Kinetic energy of v_x for (16,8), scaled.



4.3: Velocity change per step



4.4: friction force δF

Figure 4: Profiles of kinetic energy and derived frictional forces over time.

(a) Single-Wall NanoTorus			
(n, m)	l [Å]	r [Å]	N
(16,0)	1633.5	6.25	24576
(16,8)	1620.69	8.27	32256
(16,16)	943.1	10.83	24576
(b) Double-Wall NanoTori			
	inner	tube	
(n, m)	l [Å]	r [Å]	N
(16,0)	1089	6.25	16384
(16,8)	1620.69	8.27	32256
(16,16)	628.74	10.83	16384
	outer	tube	
(n, m)	l [Å]	r [Å]	N
(32,0)	1089	12.51	32768
(32,16)	1620.69	16.55	64512
(32,32)	628.74	21.67	32768

Table 1: Nanotorus geometries: chiral numbers (n, m) , mean circumference l , nanotube radius and atom count N

the velocity change is very pronounced, especially at the very beginning. Finally, the frictional force may be derived from this, see figure 4.4, and we again notice the relatively constant force felt for initial velocities below the limit τ_v . The friction force seems in general to be velocity-dependent, obvious by the small decrease over time. Note that above 0.1 Å/fs, or 60 Ghz, destruction of the buckyball is observed.

Note that in general the quality of the oscillating loop is severely degraded by friction for some velocities and chiralities. This is in contrast to the investigations of Cumings et al. [4] and considerations of Hilder et al. [10] that wall friction should in general be negligible. Note that Guo et al. found that friction is only small in the range of a few Kelvin, see [8], whereas our numerical experiments are performed at room temperature.

We want to take a closer qualitative look at this issue. In figure 5.1 a snapshot of the on-going simulation is taken and a close-up of the buckyball and the surrounding nanotorus section presented. Clearly, kinks and buckles are visible in the nanotorus' wall, triggered by the thermal motion of the atoms at room temperature.

Quantitatively, we observe that these thermal perturbations of the ideal nanotorus configurations do not diminish for infinite nanotube lengths. In figure 5.3, the mean square displacement of the nanotorus with respect to its initial configuration is again depicted for the (16,0) configuration, this time however with logarithmic scaling. We note that the displacement does not seem to go to zero for increasing nanotorus radii but to a finite value, presumed dependent on the temperature.

However, not only the thermal motion of the nanotorus' atoms create friction for the buckyball, also the interactions between the buckyball and the walls themselves generate friction. This is probably caused by Van-der-Waals forces inducing a visible kink in the tube as the buckyball passes through the tube, depicted by a snapshot of the simulation in figure 5.2. This kink is provoked by steady collisions of the buckyball against the nanotorus' wall in the potential given above in figure 3. These collisions themselves cause more instabilities and may be regarded as friction due to loss of momentum that is transferred to the walls, even in the few-Kelvin temperature case.

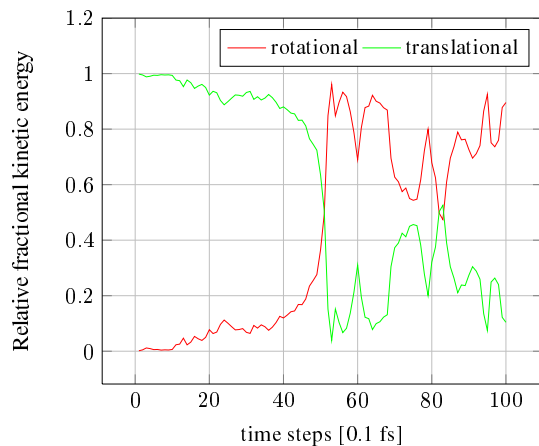
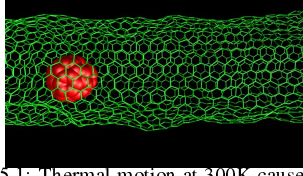


Figure 5: Relative difference to mean fractional kinetic energy per carbon atom: Wall friction induces the C_{60} to rotate around its own axis.

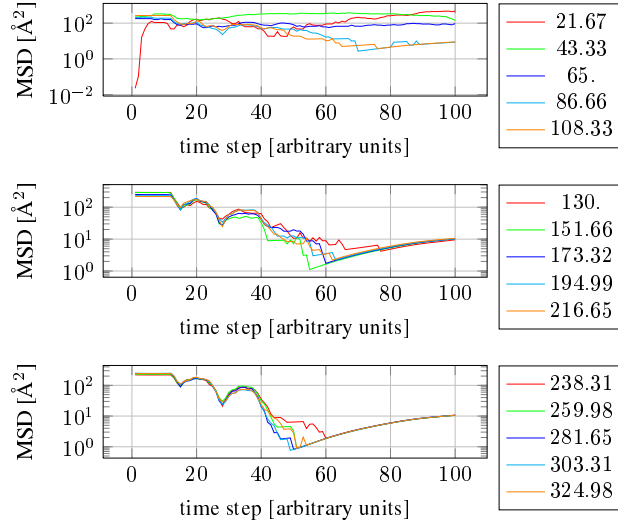
Finally, we analyse the rotational and the translational part of the kinetic energy of the buckyball, orbiting inside the nanotorus structure. The



5.1: Thermal motion at 300K causes (16, 0) nanotorus' walls to buckle



5.2: The C_{60} is forced onto its orbiting circular path by successive small collisions with the nanotorus' walls.



5.3: Thermal perturbations at 300K diminish locally in absolute strength with increasing radius, but do not vanish in the limit of infinite radius (i.e. for the infinite nanotube).

translational part is the vector sum of the velocity of each atom the buckyball consists of: $T^{trans} = \|\sum_{i=1}^{60} v_i\|_2$. The rotational part $T^{rot} = T^{tot} - T^{trans}$ is the difference to the total kinetic energy T^{tot} as the sum over the norm of each atom's velocity vector: $T^{tot} = \sum_{i=1}^{60} \|v_i\|_2$. In figure 5 this is given for the (16,0) configuration with initial velocity of 0.041 Å/fs, or roughly 30 Ghz. The wall collisions obviously cause the buckyball to rotate internally and thus to further loose translational momentum.

3.2.2 Electromagnetic properties

We have extrapolated the properties of the proposed oscillating loop or electrographic nanocoil, consisting of a nanotorus and an endohedral, orbiting C_{60} , from a purely mechanical point of view, see table 1(b). Note that we give a magnetic field strength with the notion that wall collisions might be prevented if an external magnetic field would induce a Lorentz force and thus keep the buckyball on its orbiting path. The required field strength would be quite high, however.

(a) List of initial forces employed to accelerate the buckyball

F_i [nN]	v_i [a.u.]	v_i [Å/fs]
80.1	0.0019	0.041
160.2	0.0037	0.082
320.4	0.0075	0.164
640.8	0.015	0.328
1602	0.037	0.82

(b) $q = 3e$, $r_{torus} = 2000 \text{ \AA}$, $v = 0.0019 a.u. = 0.004 \text{ \AA/fs}$, $m \approx 720 u$

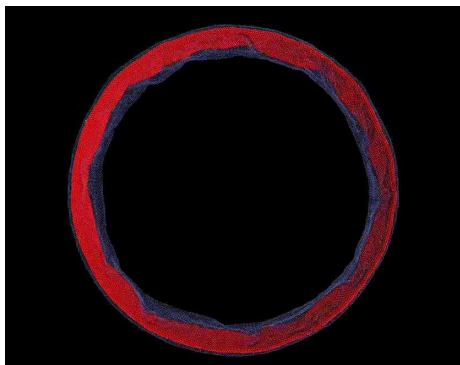
Frequency range	1-100 ghz
Synchrotron energy	0.1-10 femto joule
Radio signal strength	10^{-24} watt
Magnetic field strength	10-100 tesla

Table 2: Applied initial forces F_i at $T = 0$ ps, resulting velocities of the buckyball and an estimation of possible electromagnetic properties of the proposed electrographic nanocoil.

3.3 Multi-wall nanotori

Multi-wall nanotorus may have the advantage over single-wall tori of greater stability against impacts of the orbiting buckyball, simply due to greater mass. Even more so because the innermost torus may be used as the orbiter instead of the buckyball. This might be a possible solution to the problems found above, where successive wall collisions cause the buckyball to slow down rapidly.

Therefore, we simulate a (16,0)–(32,0) double-wall nanotorus, see table 1, where the inner torus was caused to rotate in much the same manner as the buckyball. We observe that the interactions between the tori cause a transfer of momentum to the outer torus, such that in the end both rotate at the same velocity. This is presumed to be due to the Van-der-Waals interactions but no explicit calculations have been made to investigate this issue further.



6.1: Double-wall nanotorus, where the inner torus is forced to rotate, shows induced rotation of the outer torus by frictional forces, i.e. due to van der Waals-interactions between the two tori.

3.3.1 Embedding in $(C_2H_4)_n$ matrix

In order to prevent this induced rotation of the outer torus, the multi-wall nanotorus may be embedded in a polyethylene matrix. This would have the additional benefit of protection against environmental influences on the one hand and fixing the toroidal system in its location on the other hand.

We perform initial molecular dynamics simulations on the single-wall nanotorus embedded in a

polyethylene matrix, where the total system consists of roughly 2 million atoms. Three snapshots of the initial, intermediate and final stage of the equilibration are given in figure 6 along with a snapshot highlighting the presence of cross-links between nanotorus and matrix. These are necessary to prevent transfer of momentum from the orbiting inner torus. Clearly, radial, thermally induced instabilities are greatly pronounced in contrast to the vacuum case before. Note however, that nanotorus is significantly smaller. Hence, larger radii should be investigated that might display greater wall stability but also strongly increase the computational demand to tackle these systems. Nonetheless, the thermal instabilities may necessitate cooling and thus would hinder industrial mass applications.

4 Conclusions

We have investigated carbon nanotori by molecular dynamics simulation. We focused on the implantation of carbon fullerenes to act as charge vessels – so-called metallofullerenes – in the context of possible electromagnetic applications, and on the mechanical stability, employing the well-suited Brenner potential. We find that orbiting buckyballs are probably not feasible due to friction that is caused by thermal motion of the nanotorus' wall atoms hindering the orbiting buckyball and by nanotorus–buckyball interactions causing additional kinks. We have given a brief outlook on how to overcome these issues in the context of multi-wall carbon nanotori, that encapsulate metal atoms and are themselves embedded in a polyethylene matrix. However, due to the additional matrix a realistic setup requires an immense computational load, which would call for multi-scale simulation schemes.

- [1] **Brenner, D. W.** 1990. *Physical Review B* **42** (15):9458–9471.
- [2] **Cagle, D. W., S. J. Kennel, S. Mirzadeh, J. M. Alford, and L. J. Wilson.** 1999. *Proceedings of the National Academy of Sciences of the United States of America* **96** (9):5182–5187.

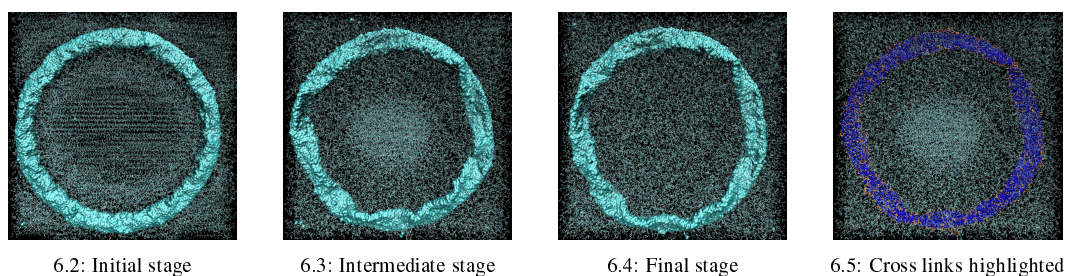


Figure 6: (16, 0) carbon nanotorus with tube radius 6.25 \AA and torus radius 86.66 \AA embedded in a polyethylene matrix with crosslinks (in orange on image at lower right) at initial (upper left), intermediate (upper right) and later stage (lower left).

- [3] Cox, B. J., N. Thamwattana, and J. M. Hill. 2006. *Proceedings of the Royal Society A* **463**:477–494.
- [4] Cumings, J., and A. Zettl. 2000. *Science* **289**:602–604.
- [5] Griebel, M., and J. Hamaekers. 2006. *In: Rietz, M., and W. Schommers.*, (ed.), *Handbook of Theoretical and Computational Nanotechnology*, vol. 9 chapter 8, p. 409–454. American Scientific Publishers.
- [6] Griebel, M., J. Hamaekers, and R. Wildenhues. 2005. *In: Sanchez, J.*, (ed.), *Proceedings 1st Nanoc-Workshop.* LABEIN, LABEIN, Bilbao, Spain. Also as INS Preprint No. 0503.
- [7] Griebel, M., S. Knapek, and G. Zumbusch. 2007. *Numerical Simulation in Molecular Dynamics*. Springer, Berlin, Heidelberg.
- [8] Guo, W., Y. Guo, H. Gao, Q. Zheng, and W. Zhong. 2003. *Physical Review Letters* **91** (12):125501.
- [9] Hilder, T. A., and J. M. Hill. 2007a. *Physical Review B* **75**:125415.
- [10] Hilder, T. A., and J. M. Hill. 2007b. *Journal of Applied Physics* **101**:064319.
- [11] Hirahara, K., K. Suenaga, S. Bandow, H. Kato, T. Okazaki, H. Shinohara, and S. Iijima. 2000. *Physical Review Letters* **85** (25):5384–5387.
- [12] Huhtala, M., A. Kuronen, and K. Kaski. 2002. *Computer Physics Communications* **146**:30–37.
- [13] Kaka, S., M. R. Puffall, W. H. Rippard, T. J. Silva, S. E. Russek, and J. A. Katine. 2005. *Nature* **437**:389–392.
- [14] Lee, J., H. Kim, S.-J. Kahng, G. Kim, Y.-W. Son, J. Ihm, H. Kato, Z. W. Wanz, T. Okazaki, H. Shinohara, and Young Kuk. 2002. *Nature* **415**:1005–1008.
- [15] Legoas, S. B., V. R. Coluci, S. F. Braga, P. Z. Coura, S. O. Dantas, and D. S. Galvão. 2004. *Nanotechnology* **15**:S184–S189.
- [16] Liu, C., H. B. Chen, and J. W. Wing. 2008. *Journal of Physics: Condensed Matter* **20**:015206.
- [17] Liu, J., H. Dai, J. H. Hafner, D. T. Colbert, R. E. Smalley, S. J. Tans, and C. Dekker. 1997. *Nature* **385**:780–781.
- [18] Liu, L., G. Y. Guo, C. S. Jayanthi, and S. Y. Wu. 2002. *Physical Review Letters* **88** (21):217206.
- [19] Lu, D., Y. Li, U. Ravaioli, and K. Schulten. 2005. *Physical Review Letters* **95**:246801.
- [20] Ma, C.-C., Y. Zhao, C.-Y. Yam, G. Chen, and Q. Jiang. 2005. *Nanotechnology* **16** (8):1253–1264.

- [21] **Martel, R., H. R. Shea, and P. Avouris.** 1999a. *Journal of Physical Chemistry* **103** (36):7551–7556.
- [22] **Martel, R., H. R. Shea, and P. Avouris.** 1999b. *Nature* **398**:299–300.
- [23] **Muster, J., M. Burghard, S. Roth, G. S. Duesberg, E. Hernández, and A. Rubio.** 1998. *Journal of Vacuum Science and Technology B – Microelectronics and Nanometer Structures* **16**:2796–2800.
- [24] **Rocha, C. G., M. Pacheco, Z. Barticevic, and A. Latgé.** 2004. *Physical Review B* **70** (23):233402.
- [25] **Ruoff, R. S., J. Tersoff, D. C. Lorents, S. Subramoney, and B. Chan.** 1993. *Nature* **264**:514–516.
- [26] **Shinohara, H.** 2000. *Rep. Prog. Phys.* **63**:843–892.
- [27] **Suenaga, K., T. Tencé, C. Mory, C. Colliex, H. Kato, T. Okazaki, H. Shinohara, K. Hirahara, S. Bandow, and S. Iijima.** 2000. *Science* **290** (5500):2280–2282.
- [28] **Takata, M., B. Umeda, E. Nishibori, M. Sakata, Y. Saito, M. Ohno, and H. Shinohara.** 1995. *Nature* **377**:46–49.
- [29] **Tsai, C., F. L. Shyu, C. W. Chiu, C. P. Chang, R. B. Chen, and M. F. Lin.** 2004. *Physical Review B* **70**:075411.
- [30] **Tuzun, R. E., D. W. Noid, B. G. Sumpter, and R. C. Merkle.** 1997. *Nanotechnology* **8** (3):112–118.
- [31] **Zhang, Z., Z. Yang, J. Wang, X. anf Yuan, H. Zhang, M. Qiu, and J. Peng.** 2005. *Journal of Physics: Condensed Matter* **17**:4111–4120.
- [32] **Zhao, Y., C.-C. Ma, G. Chen, and Q. Jiang.** 2003. *Physical Review Letters* **91** (17):175504.